Supplementary Materials

This section provides supplementary visualizations related to the data and results. The scatter plot in **Error! Reference source not found.Error! Reference source not found.** illustrates the temporal distribution of in-situ Chl-*a* matchups, colour-coded based on corresponding satellite imagery. **Error! Reference source not found.** displays a heatmap emphasizing the significance of each scheme in each data category with respect to in-situ Chl-*a* concentrations, with colour variations representing different R^2 performances. Three tables are also presented in this section.

offers quantitative details of the in-situ data utilized, while **Error! Reference source not found.** describes each of the atmospheric correction processors employed. **Error! Reference source not found.** delivers a comprehensive description of the RS-derived Chl-*a* models developed, along with their performance metrics.

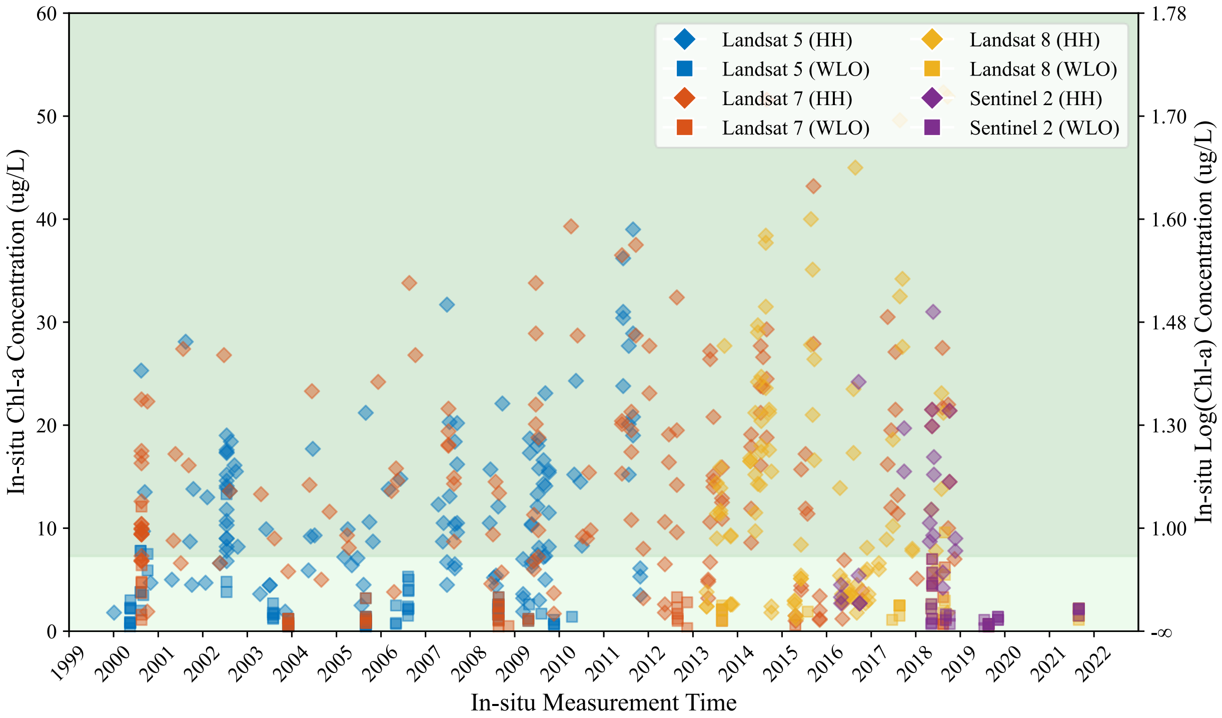

Figure S Time series plot of in-situ data, displaying Hamilton Harbour (HH, diamond markers) and Western Lake Ontario (WLO, square markers) alongside Landsat 5 (blue), 7 (red), 8 (yellow), and Sentinel-2 (purple) matchups. The green background represents classes of oligotrophic/mesotrophic and eutrophic/hypereutrophic based on Carlson's Trophic State Index (TSI). Two outlier concentrations of 137 and 80 μg/L are excluded for better visual presentation.

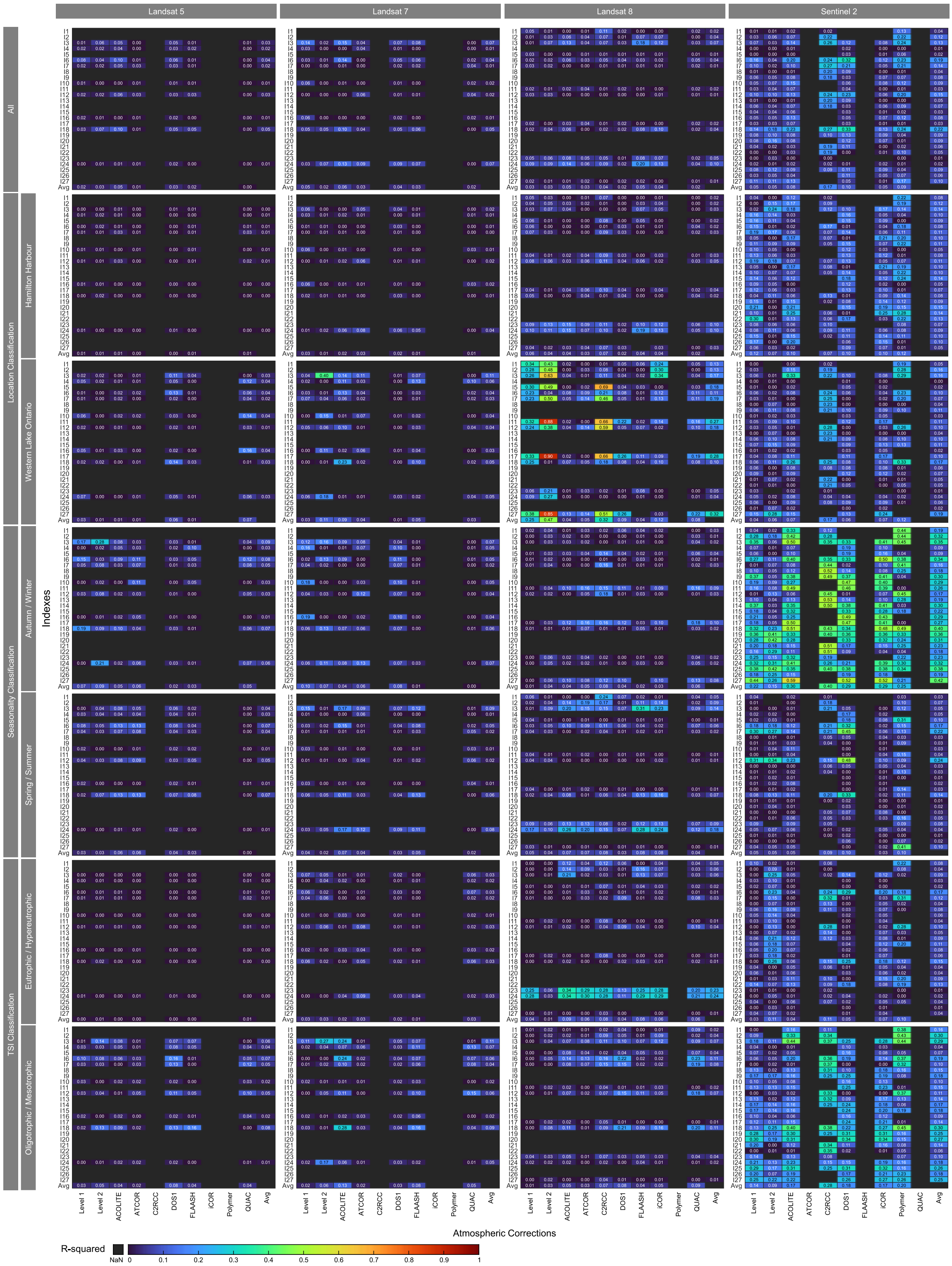

Figure S Heatmaps of R^2 between in-situ Chl-a concentrations and corresponding index values of co-located pixels across various schemes and subcategories. Warmer colours indicate higher R^2 (better performance), while colder ones signify lower RBlack cells indicate N/A values.

Table S Descriptive statistics of the in-situ data categorized based on seasonality, study location and Carlson's Trophic State Index (TSI).

	Location Category	Seasonality Category	TSI Category

	All	HH	WLO	Autumn/Winter	Spring/Summer	Oligotrophic/Mesotrophic	Eutrophic/Hypereutrophic
Count or 'n'	600	410	190	132	468	305	295
Frequency (%)	100%	68%	32%	22%	78%	51%	49%
Mean (μg/L)	10.5	14.3	2.2	9.6	10.7	2.9	18.3
Std. Deviation (μg/L)	11.3	11.8	2.0	10.0	11.7	1.9	11.6
Minimum (μg/L)	0.2	1.0	0.2	0.2	0.3	0.2	7.3
Maximum (μg/L)	137.0	137.0	13.3	51.9	137.0	7.2	137.0

Table SAtmospheric correction possessors utilized in this study. Level-2 products of Landsat 5 and 7 (LEDAPS- and LaSRC-corrected) are readily available for download, therefore excluded from the table below.

Name	**Supported Sensors***	**Input Products**	**Output Products**	**Processing Environment**	**Pros**	**Cons**	**Main Application**	**Processing Speed**	**Latest Version (Release Year)**	**Key References**
ACOLITE	TM, ETM+, OLI, MSI	DN, TOA reflectance and ancillary data	TOA reflectance, surface level reflectance, normalized water-leaving reflectance, Rayleigh corrected reflectance, remote sensing reflectance, TSM concentration, turbidity, Chl-*a* concentration, and more	Python Graphical User Interface (GUI) and Python Command Line Interface (CLI)	Freely available, supports many sensors, flexible and customizable, user-friendly, glint correction, masking, Q/A forum support, batch mode	Limited to the processing of coastal and inland water	Aquatic	Moderate/Slow (depending on the selected outputs)	20221114.0 (2022)	[1,2]
ATCOR 3	TM, ETM+, OLI, MSI	DN, TOA reflectance, DEMs and ancillary data	TOA reflectance, ground reflectance, surface temperature, water vapour map	Geomatica (CATALYST), IDL, and Python	Supports many sensors, flexible and customizable, haze removal, topographic correction, cirrus removal, batch mode	Commercial, manual parameter selection and adjustment	Land, coastal, and water	Fast	9.4.0 (2022)	[3,4]
C2RCC	OLI, MSI	TOA reflectance and ancillary data	Surface reflectance, normalized water-leaving reflectance (ρ_{wn}), Chl-*a* concentration, TSM concentration	Plugin to the ESA SNAP	Freely available, designed for water, open-source code, based on machine learning and neural	Limited to a few sensors, unsuitable for non-water applications	Coastal and inland water	Moderate (depending on the selected outputs)	-	[5,6]

			and their related uncertainties and more		network, correction for many factors (gaseous absorption, air pressure, etc.)					
DOS1	TM, ETM+, OLI, MSI	DN, TOA Reflectance	Surface reflectance	Plugin to the QGIS (Semi-Automatic Classification Plugin, SCP)	Freely available, easy to implement, suitable for a wide range of sensors, open source	Simplifying assumptions, less accurate for complex atmospheric conditions	Land, coastal, and water	Fast	7.10.11 (2023)	[7,8]
FLAASH	TM, ETM+, OLI	Radiance in BIL or BIP format and ancillary data	Apparent reflectance (upscaled to 10,000), water vapour, cloud map (only for hyperspectral input)	Plugin to the ENVI, stand-alone C++ module	Reliable, supports a wide range of sensors, available for multispectral and hyperspectral sensors, water and aerosol retrieval and cloud masking	Commercial, manual parameter selection and adjustment	Land, coastal, and water	Slow	4.7 (2009)	[9,10]
iCOR (previously known as OPERA)	OLI, MSI	TOA reflectance	BOA reflectance	Plugin to the ESA SNAP	Freely available (basic version), generic, requires few input parameters, available for spaceborne, airborne and drone images, correction for adjacency effects	Limited sensor support, limited output products	Land, coastal, and water	Moderate	3.0.0	[11,12]
Polymer	MSI	TOA reflectance and ancillary data	Water reflectance and more	Python CLI	Freely Available Flexible and robust, Q/A forum support, correction for sunglint, batch mode, land mask, cloud mask	Unsuitable for non-water applications, user-unfriendly	Water	Moderate	4.16 (2023)	[13,14]
QUAC	TM, ETM+, OLI	DN, apparent reflectance or radiance	Apparent reflectance (upscaled to 10,000)	Plugin to the ENVI, stand-alone C++ module	Easy to use, supports a wide range of sensors, does not require ancillary data, does not require knowledge of sensor	Commercial, less accurate, unsuitable for water-only scenes	Land, coastal, and water	Fast	-	[15]

					metadata, available for hyperspectral and multispectral imagery					
Sen2Cor	MSI	TOA reflectance and ancillary data	BOA reflectance	Plugin to the ESA SNAP and Python CLI	Freely available, reliable for MSI, correction for terrain and cirrus, and aerosol optical thickness, water vapour, scene classification map and quality indicators for cloud and snow probabilities	Limited to MSI	Land, coastal, and water	Moderate	2.11.00 (2022)	[16,17]

* Only limited to the list of sensors used in this study. Abbreviations in alphabetical order: BOA: Bottom-of-Atmosphere, DN: Digital Number, TOA: Top-of-Atmosphere.

Table SSummary of RS-derived Chl-a models across satellites and data categories. L5 = Landsat 5, L7 = Landsat 7, L8 = Landsat 8 and S2 = Sentinel-2.

Model	AC	RS-Derived Chl-*a*	n	RMSE (µg/L)	RMSLE	Bias	MAE	MAPE (%)	MDAPE (%)	ε (%)	β (%)	R^2
M_{L5-All}	ACOLITE	$Chla_{RS}$= -14.00×I_{18} + 11.85	201	11.25	0.41	1.53	2.12	139.00	59.80	87.45	39.15	0.35
M_{L5-HH}	QUAC	$Chla_{RS}$= 4.90×I_{7} + 5.47	123	13.23	0.31	1.25	1.74	84.13	41.30	54.46	24.94	0.01
M_{L5_WLO}	QUAC	$Chla_{RS}$= 1.03×I_{4} + 1.59	82	1.82	0.21	1.02	1.43	36.10	26.69	28.86	12.31	0.19
M_{L5-AW}	Level-2 (LEDAPS)	$Chla_{RS}$= -25.20×I_{3} + 31.74	42	5.35	0.39	1.35	2.08	123.11	51.80	94.68	25.01	0.30
M_{L5-SS}	ATCOR	$Chla_{RS}$= -19.68×I_{18} + 14.74	161	12.15	0.39	1.44	1.99	126.12	50.65	73.14	33.14	0.38
M_{L5-EH}	QUAC	$Chla_{RS}$= 11.55×I_{12} + 13.89	93	14.12	0.21	1.15	1.46	43.68	37.41	41.45	12.30	0.00
M_{L5-OM}	DOS1	$Chla_{RS}$= -2.48×I_{6} + 7.53	112	1.68	0.22	1.08	1.54	48.03	42.24	56.64	12.38	0.25
M_{L7-All}	Level-2 (LEDAPS)	$Chla_{RS}$= -15.52×I_{3} + 26.41	216	9.64	0.49	1.56	2.48	202.12	61.20	107.78	24.78	0.10
M_{L7-HH}	ACOLITE	$Chla_{RS}$= 500.40×I_{24} + 10.26	160	8.99	0.35	1.26	1.80	109.47	41.75	52.45	10.17	0.04
M_{L7-WLO}	Level-2 (LEDAPS)	$Chla_{RS}$= -19.41×I_{3} + 21.53	57	1.51	0.20	1.02	1.47	40.61	34.53	38.17	11.35	0.38
M_{L7-AW}	Level-1	$Chla_{RS}$= -47.12×I_{4} + 28.64	39	10.12	0.52	1.72	2.68	210.25	69.72	189.76	59.91	0.19
M_{L7-SS}	Level-2 (LEDAPS)	$Chla_{RS}$= -10.74×I_{3} + 22.04	178	9.33	0.48	1.51	2.35	192.44	56.90	83.35	22.78	0.07
M_{L7-EH}	ATCOR	$Chla_{RS}$= 0.01×I_{24} + 17.57	122	7.75	0.18	1.08	1.42	38.36	31.73	40.00	9.08	0.08
M_{L7-OM}	Level-2 (LEDAPS)	$Chla_{RS}$= -15.79×I_{3} + 18.52	94	1.69	0.24	1.11	1.62	57.22	45.48	63.44	15.65	0.30
M_{L8-All}	FLAASH	$Chla_{RS}$= 0.08×I_{24} + 3.64	115	12.29	0.49	1.57	2.49	204.36	66.45	122.72	46.81	0.08
M_{L8-HH}	FLAASH	$Chla_{RS}$= 0.08×I_{24} + 5.66	96	12.67	0.44	1.44	2.21	167.45	60.91	100.66	26.44	0.08
M_{L8-WLO}	Level-1	$Chla_{RS}$= 23.72×I_{1} - 24.32	24	1.39	0.18	1.13	1.39	38.71	25.19	31.38	14.02	0.39
M_{L8-AW}	C2RCC	$Chla_{RS}$= 4.72×I_{7} - 0.67	32	11.33	0.46	1.53	2.38	175.36	65.65	102.25	53.15	0.14
M_{L8-SS}	FLAASH	$Chla_{RS}$= -27.09×I_{3} + 36.80	93	11.72	0.45	1.46	2.15	161.20	64.74	103.30	36.31	0.23
M_{L8-EH}	ACOLITE	$Chla_{RS}$= -41.56×I_{3} + 53.14	62	11.58	0.21	1.15	1.49	49.88	39.97	45.99	13.32	0.26
M_{L8-OM}	QUAC	$Chla_{RS}$= -0.80×I_{6} + 4.22	63	1.25	0.18	1.08	1.41	39.04	32.75	39.32	10.32	0.24
M_{S2-All}	DOS1	$Chla_{RS}$= -17.38×I_{18} + 9.50	51	6.19	0.38	1.36	2.00	119.66	54.24	76.54	39.85	0.36
M_{S2-HH}	Polymer	$Chla_{RS}$= 27.64×I_{2} - 0.14	24	6.97	0.31	1.24	1.79	85.43	44.74	68.26	15.53	0.16
M_{S2-WLO}	ACOLITE	$Chla_{RS}$= -5.84×I_{3} + 7.99	27	1.10	0.17	1.03	1.36	35.05	24.10	28.30	0.85	0.37
M_{S2-AW}	ACOLITE	$Chla_{RS}$= -17.57×I_{18} + 15.51	18	5.95	0.37	1.30	1.68	117.28	26.20	35.50	10.84	0.49
M_{S2-SS}	DOS1	$Chla_{RS}$= -57.12×I_{12} + 12.11	33	5.11	0.37	1.16	2.04	105.54	58.21	104.07	2.28	0.32
M_{S2-EH}	DOS1	$Chla_{RS}$= 22.01×I_{18} + 17.93	16	5.50	0.15	1.06	1.32	29.56	22.51	24.37	13.08	0.32
M_{S2-OM}	ACOLITE	$Chla_{RS}$= -5.01×I_{3} + 7.08	35	1.16	0.16	1.03	1.36	33.36	28.22	36.06	5.66	0.52

References

1. Vanhellemont, Q. Adaptation of the Dark Spectrum Fitting Atmospheric Correction for Aquatic Applications of the Landsat and Sentinel-2 Archives. *Remote Sens. Environ.* **2019**, *225*, 175–192, doi:10.1016/j.rse.2019.03.010.
2. Vanhellemont, Q.; Ruddick, K. Atmospheric Correction of Metre-Scale Optical Satellite Data for Inland and Coastal Water Applications. *Remote Sens. Environ.* **2018**, *216*, 586–597, doi:10.1016/j.rse.2018.07.015.
3. Richter, R.; Schläpfer, D. Atmospheric/Topographic Correction for Satellite Imagery. In : DLR Report DLR-IB 565-02/*DLR Rep. DLR-IB* **2011**, *565*, 202.
4. Richter, R.; Schläpfer, D.; Center, G.D.L.R.— G.A. Atmospheric/Topographic Correction for Satellite Imagery (ATCOR-2/3 User Guide, Version 8.2.1, February 2013). **2013**, *3*, 224.
5. Brockmann, C.; Doerffer, R.; Peters, M.; Stelzer, K.; Embacher, S.; Ruescas, A. Evolution of the C2RCC Neural Network for Sentinel 2 and 3 for the Retrieval of Ocean Colour Products in Normal and Extreme Optically Complex Waters. In Proceedings of the European Space Agency, (Special Publication) ESA SP; 2016; Vol. SP-740, p. 54.
6. Schiller, H.; Doerffer, R. Neural Network for Emulation of an Inverse Model Operational Derivation of Case II Water Properties from MERIS Data. *Int. J. Remote Sens.* **1999**, *20*, 1735–1746, doi:10.1080/014311699212443.
7. Congedo, L. Semi-Automatic Classification Plugin Semi-Automatic Classification Plugin Documentation. **2017**, *4*, 3–206.
8. Congedo, L. Semi-Automatic Classification Plugin: A Python Tool for the Download and Processing of Remote Sensing Images in QGIS. *J. Open Source Softw.* **2021**, *6*, 3172, doi:10.21105/joss.03172.
9. ENVI ENVI Atmospheric Correction Module: QUAC and FLAASH User's Guide. **2009**, *4*, 44.
10. Felde, G.W.; Anderson, G.P.; Cooley, T.W.; Matthew, M.W.; Adler-Golden, S.M.; Berk, A.; Lee, J. Analysis of Hyperion Data with the FLAASH Atmospheric Correction Algorithm. In Proceedings of the IGARSS 2003. 2003 IEEE International Geoscience and Remote Sensing Symposium. Proceedings (IEEE Cat. No.03CH37477); IEEE, 2003; Vol. 1, pp. 90–92.
11. De Keukelaere, L.; Sterckx, S.; Adriaensen, S.; Knaeps, E.; Reusen, I.; Giardino, C.; Bresciani, M.; Hunter, P.; Neil, C.; Van der Zande, D.; et al. Atmospheric Correction of Landsat-8/OLI and Sentinel-2/MSI Data Using ICOR Algorithm: Validation for Coastal and Inland Waters. *Eur. J. Remote Sens.* **2018**, *51*, 525–542, doi:10.1080/22797254.2018.1457937.
12. Wolters, E.; Toté, C.; Sterckx, S.; Adriaensen, S.; Henocq, C.; Bruniquel, J.; Scifoni, S.; Dransfeld, S. Icor Atmospheric Correction on Sentinel-3/OLCI over Land: Intercomparison with Aeronet, Radcalnet, and Syn Level-*Remote Sens.* **2021**, *13*, 1–26, doi:10.3390/rs13040654.
13. Steinmetz, F.; Deschamps, P.-Y.; Ramon, D. Atmospheric Correction in Presence of Sun Glint: Application to MERIS. *Opt. Express* **2011**, *19*, 9783, doi:10.1364/oe.19.009783.
14. Steinmetz, F.; Ramon, D. Sentinel-2 MSI and Sentinel-3 OLCI Consistent Ocean Colour Products Using POLYMER. In Proceedings of the Remote Sensing of the Open and Coastal Ocean and Inland Waters; Frouin, R.J., Murakami, H., Eds.; SPIE, October 30 2018; p. 13.
15. Bernstein, L.S. Quick Atmospheric Correction Code: Algorithm Description and Recent Upgrades. *Opt. Eng.* **2012**, *51*, 111719, doi:10.1117/1.oe.51.11.111719.
16. Main-Knorn, M.; Pflug, B.; Louis, J.; Debaecker, V.; Müller-Wilm, U.; Gascon, F. Sen2Cor for Sentinel-In Proceedings of the Image and Signal Processing for Remote Sensing XXIII; Bruzzone, L., Bovolo, F., Benediktsson, J.A., Eds.; SPIE, October 4 2017; Vol. 10427, p. 3.
17. Louis, J.; Debaecker, V.; Pflug, B.; Main-Knorn, M.; Bieniarz, J.; Mueller-Wilm, U.; Cadau, E.; Gascon, F. Sentinel-2 SEN2COR: L2A Processor for Users. In Proceedings of the European Space Agency, (Special Publication) ESA SP; 2016; Vol. SP-740, pp. 1–8.